Synthesis and anti-inflammatory activity of a chimeric recombinant superoxide dismutase: SOD2/3

Bifeng Gao, Sonia C. Flores, Jonathan A. Leff, Swapan K. Bose, and Joe M. McCord
Webb-Waring Institute, University of Colorado Health Sciences Center, Denver, Colorado 80262

Gao, Bifeng, Sonia C. Flores, Jonathan A. Leff, Swapan K. Bose, and Joe M. McCord. Synthesis and anti-inflammatory activity of a chimeric recombinant superoxide dismutase: SOD2/3. *Am J Physiol Lung Cell Mol Physiol* 284: L917–L925, 2003. First published January 10, 2003; 10.1152/ajplung.00374.2002.—External surfaces of cells are normally protected by extracellular superoxide dismutase, SOD3, which binds to polyanions such as heparan sulfate. We constructed a fusion gene encoding a chimeric SOD consisting of the mature human mitochondrial SOD2 plus the COOH-terminal 26-amino acid heparin-binding "tail" from SOD3. This tail is responsible for the enzyme's affinity for endothelial surfaces. The fusion gene was expressed in *Escherichia coli*, and the fully active enzyme SOD2/3 was purified. Although native SOD2 has no affinity for heparin, SOD2/3 binds to a heparin-agarose column. In a rat model of acute lung injury induced by intratracheal instillation of IL-1, SOD2/3, SOD2, and denatured SOD2/3 showed 92%, 13.8%, and 0% reduction of lung leak, respectively. Only SOD2/3 prevented neutrophil accumulation. In the carrageenan-induced foot edema model in the rat, SOD2/3 reduced edema by 62% ($P < 0.003$) at a dose in which native SOD2 produced no significant effect. Thus SOD2/3 appears to have properties as a therapeutic anti-inflammatory agent that are greatly superior to other available forms of the enzyme.

inflammation; lung injury; interleukin-1; free radicals; oxidative injury

ACTIVE OXYGEN SPECIES ARE involved in the pathogenesis of a variety of diseases. In many laboratory models and in a few clinical trials, superoxide dismutase (SOD) has proven therapeutically useful in protecting injured tissues from one of these active oxygen species, the superoxide radical (24). The ability of SOD to protect tissues against any particular insult (ischemia, inflammation, hyperoxia, etc.) depends on several parameters such as its rate of plasma clearance (30), ability to equilibrate between extracellular fluid compartments (36), and the ability to closely approach negatively charged cell surfaces (29). Other enzymes that are part of the cell's arsenal against these active oxygen species include catalase and glutathione peroxidase, which eliminate H_2O_2.

In humans, three isozymes of SOD have been extensively characterized: the cytosolic Cu,Zn-SOD or SOD1, a 32-kDa dimer (27); the mitochondrial Mn-SOD or SOD2, an 89-kDa tetramer (26); and an extracellular-SOD or SOD3, a 135-kDa tetrameric glycoprotein (20). SOD3 is also a cuprozinc enzyme, genetically related to SOD1, and is found in a number of tissues but at a much lower concentration than either of the other two enzymes (21, 22). It is, however, the major SOD in extracellular fluids. SOD3 is found as three different forms: SOD3-A with no heparin affinity, SOD3-B with low heparin affinity, and SOD3-C with high heparin affinity. Sandstrom et al. (39) have suggested that forms A and B are generated by proteolytic cleavage of a COOH-terminal "tail" found intact on the C form. The highly hydrophilic, positively charged nature of this COOH-terminal tail imparts the high heparin affinity that allows the enzyme to be largely bound to heparan sulfate on endothelial surfaces (10, 39, 41).

Under normal circumstances, intracellularly generated superoxide is efficiently handled by the cytosolic SOD1 and mitochondrial SOD2. However, under pathological conditions, large amounts of superoxide and its metabolites may be produced (8, 23). In this case, one major site of oxidant attack is endothelial cell surfaces, where membrane perturbation leading to cell death (possibly through apoptosis or programmed cell death) may be induced. Therefore, we propose that the plasma membranes of vascular endothelial cells and parenchymal cells may require additional protection when there is excessive production of these species. Surface-bound SOD3 normally protects endothelial cell surfaces from superoxide attack. However, we have shown that proteases released by inflammatory cells can cleave the SOD3 tail, allowing the enzyme to become soluble and rendering the endothelium susceptible to superoxide attack (28). To protect the endothelium, pharmacological efforts have concentrated on utilizing the cytosolic SOD1, which unfortunately has undesirable pharmacological properties: a short plasma half-life (6–15 min, depending on species) following intravenous injection with rapid clearance by the kidneys and a net negative charge at physiological pH. This net negative charge precludes close contact with cellular surfaces (29) and/or movement into interstitial spaces (36). In contrast, SOD2 is nearly uncharged at physiological pH and has a longer plasma half-life (~4 h) (1). In an isolated, perfused heart

---

Address for reprint requests and other correspondence: J. M. McCord, Box C-321, Univ. of Colorado Health Sciences Center, 4200 E. Ninth Ave., Denver, CO 80262 (E-mail: joe.mccord@uchsc.edu).

model, SOD2 is more protective and equilibrates more quickly than SOD1 (36). SOD3 may have a substantial advantage over SOD1 and SOD2 because of its ability to bind to the endothelium. Unfortunately, the SOD3 cDNA has resisted attempts at high-level recombinant expression in bacterial or yeast vectors; it has only been available from an expensive, labor-intensive, low-yield mammalian expression system, Chinese hamster ovary cells (44). A recent study (11) reports expression of human recombinant (hr) SOD3 in *E. coli* as insoluble inclusion bodies. The solubilized, refolded, purified enzyme was ∼30% active from *E. coli* and only ∼7% active from the baculovirus system. Purification yields were not reported, and the products were not tested for heparin affinity. Thus hrSOD3 has not been readily available for study.

We report here the construction of a chimeric fusion SOD that combines the desirable features of both SOD2 and SOD3: the coding sequence from the mature (i.e., minus the mitochondrial targeting signal sequence) human SOD2 followed by the 26-residue COOH-terminal tail from human SOD3. In addition, to obtain high-level expression of this mutant enzyme, we have utilized a novel expression vector designed and constructed for this purpose (7). Characterization of the enzyme and its physiological properties in two laboratory models of inflammation are also described.

MATERIALS AND METHODS

Enzymes and Chemicals

All enzymes used for manipulation of DNA were from New England Biolabs or Stratagene. Sequencing materials were obtained from United States Biochemicals. Purified human recombinant SOD1 and SOD2 were generously provided by Biotechnology General (Iselin, NJ). Human recombinant interleukin-1α (IL-1α) was kindly provided by Hoffmann-La-Roche (Nutley, NJ). Ketamine hydrochloride was from Parke-Davis (Morris Plains, NJ), xylazine was from Haver (New York, NY), ^{125}I-labeled bovine serum albumin (^{125}I-BSA) was from ICN Radiochemicals (Irvine, CA), and heparin sulfate was from Eli Lilly (Indianapolis, IN). All other chemicals were from Sigma (St. Louis, MO).

Manipulation of DNA

Isolation of plasmid DNA, preparation of DNA fragments, and DNA ligations were carried out as described by Sambrook et al. (38). Plasmid transformation was performed as described (9). Screening of putative recombinant colonies was done using PCR unless specified otherwise. Restriction enzyme digestions and DNA sequencing were carried out according to manufacturer's specifications. PCR was performed according to manufacturer's specifications (Perkin Elmer/Cetus).

E. Coli Strains

E. coli UT5600 (New England Biolabs) is a strain deficient in an outer membrane protease that cleaves between sequential basic amino acids (6). *E. coli* QC774 is deficient in both *sodA* and *sodB*. It was originally created by Carlioz and Touati (3) and was a gift of Dr. Bernard Weiss.

pGB1 Expression Vector

We have previously described the construction of the expression vector used in these studies (7). It contains the oxygen- and oxidant-sensitive *E. coli* MnSOD (*sodA*) promoter as well as both 5′-untranslated and transcriptional termination sequences plus a synthetic linker containing two restriction enzyme cloning sites, *Nsi*I and *Sac*I. The vector also contains the gene for β-lactamase, which confers ampicillin resistance to the host bacterium and provides a selectable marker. High level of expression can be achieved by exposure to the superoxide-generating agent paraquat (methyl viologen) as the inducer. The highest expression is induced by 20 μM paraquat, with the recombinant protein approaching 50% of total soluble protein produced by the host.

Construction of pGB1-sod2

A fragment of the human *sod2* cDNA encoding amino acids 25–222 (mature SOD2, minus the mitochondrial transit peptide) was obtained from a human placental cDNA library by PCR amplification and cloned into pBlueScript KS+ (Stratagene). The sequence of the primers used for the PCR amplification was as follows: forward primer, GGAATTCATG-CATAAGCACAGCCTCCCCGAC; reverse primer, CGAGC-TCTTACCCGGGCTTTTTGCAAGCCATGTA. The forward primer contains an *Eco*RI site (double underline) upstream of an *Nsi*I (single underline) restriction endonuclease site. The *Nsi*I sequence contains an ATG start codon. The reverse primer contains a *Sac*I site (single underline) immediately upstream from the translational stop codon. An *Xma*I site (isoschizomer of *Psp*AI, double underline) was positioned immediately downstream from the stop codon. After amplification and cloning, the *Sac*I and *Xma*I sites were positioned downstream and upstream, respectively, from the translational stop codon. After corroborating the cloned *sod2* cDNA sequence, the recombinant vector was digested with *Nsi*I and *Sac*I restriction endonucleases, and the resultant fragment was recovered from a low-melting point agarose gel (Nu Sieve, FMC Bioproducts, Rockland, ME). This fragment was then subcloned into *Sac*I/*Xma*I-digested pGB1. The recombinant plasmid was designated as pGB1-*sod2*, and its restriction map is shown in Fig. 1. The SOD2 translated from this construct would begin with met-his residues, followed by residues 25–222 of the human SOD2 sequence, followed by pro-gly residues (the first residues of the SOD3 26-residue tail) introduced by the cloning strategy to create an *Xma*I site to permit subsequent construction of the chimeric *sod2/3* gene.

Construction of Chimeric pGB1-sod2/3

To begin construction of the chimeric *sod2/3* gene, an ∼83-bp cDNA fragment encoding the COOH-terminal 26-amino acids from SOD3 was gel purified after *Xma*I/*Sac*I double digestion of a *sod3* cDNA-containing recombinant plasmid provided by Dr. Y. S. Ho. Plasmid pGB1-*sod2* was digested with *Xma*I and *Pst*I, and the large 3.4-kbp resultant fragment was gel purified. In a separate reaction, pGB1-*sod2* was digested with *Sac*I and *Pst*I to generate two fragments, a 3.4-kb and a smaller 306-bp fragment. After gel purification, the small *Sac*I/*Pst*I fragment and the large 3.4-kb *Xma*I/*Pst*I fragment from pGB1-*sod2* were ligated to the *Xma*I/*Sac*I tail fragment from *sod3* by incubation overnight at 15°C in the presence of T$_4$ DNA ligase according to the manufacturer's specifications. The new recombinant plasmid was designated as pGB1-*sod2/3*.
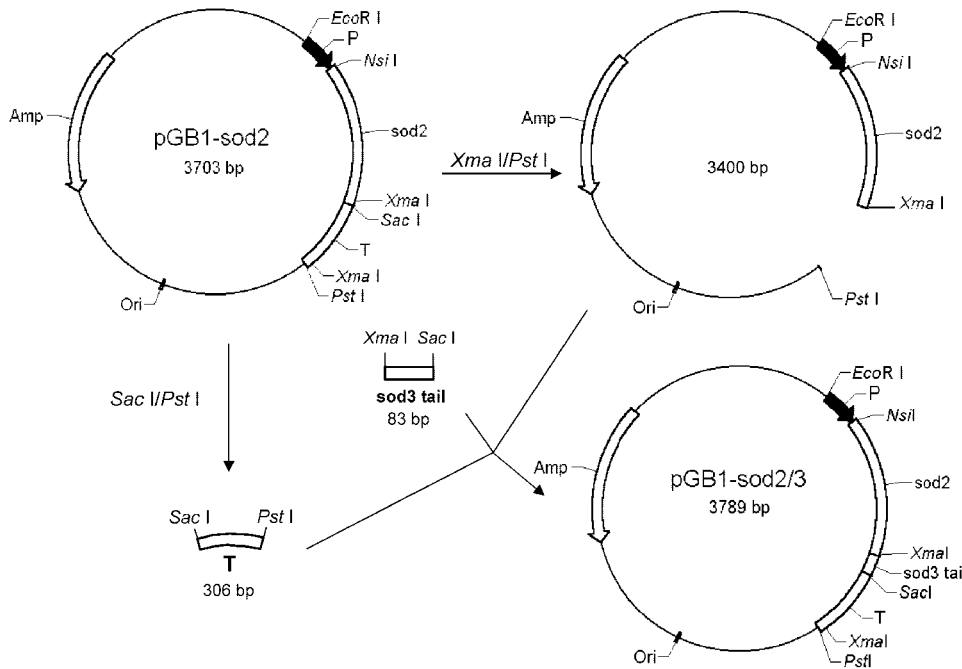
Fig. 1. Construction of plasmid encoding human superoxide dismutase (SOD)2/3. The DNA fragment encoding the human SOD3 COOH-terminal 26-amino acid basic peptide is designated sod3 tail. Amp, ampicillin-resistance gene; Ori, origin of replication; P, promoter sequence; T, termination sequence.

Figure 1 illustrates the construction scheme for this plasmid. Figure 2 represents the nucleotide and deduced amino acid sequences of the product expressed by pGB1-*sod2/3*.

Expression and Purification of SOD2/3

After transformation of competent *E. coli* UT5600 (protease-deficient) cells, positive clones were identified and cultured at 37°C for 12 h in LB (Luria-Bertani) medium supplemented with 200 μM MnSO$_4$ and 20 μM paraquat. After centrifugation, the harvested cells were lysed by sonication in a 0.1 M sodium carbonate, 0.6 M NaCl, pH 10.5 buffer. The cell debris was removed from the cell lysate by centrifugation for 30 min at 10,000 g. The supernatant was collected and subjected to heat treatment at 65°C for 10 min. The sample was cooled immediately in an ice bath and centrifuged for 10 min at 10,000 g to remove precipitated protein. Ultrafiltration with Diaflo PM-30 membrane was used to concentrate the supernatant. The sample was then chromatographed through a 15 × 700-mm column of Sephacryl S-200. Fractions were collected and assayed for SOD activity as described (5, 27). Higher-molecular-weight fractions exhibiting SOD activity were pooled, concentrated by ultrafiltration, and diluted with 10 mM Tris·HCl, pH 7.4, 0.15 M NaCl buffer. This sample was then applied to a heparin-agarose column. Fractions from this column were eluted by using a 0.15–1 M NaCl linear gradient in the buffer described above and subsequently assayed for SOD activity. Pooled fractions were then subjected to ultrafiltration, changing the buffer

The sequence of chimeric SOD2/3

```
    ATG CAT AAG CAC AGC CTC CCC GAC CTG CCC TAC GAC TAC GGC GCC CTG GAA CCT CAC ATC AAC GCG CAG ATC ATG CAG CTG CAC CAC AGC
  1 MET His Lys His Ser Leu Pro Asp Leu Pro Tyr Asp Tyr Gly Ala Leu Glu Pro His Ile Asn Ala Gln Ile Met Gln Leu His His Ser

    AAG CAC CAC GCG GCC TAC GTG AAC AAC CTG AAC GTC ACC GAG GAG AAG TAC CAG GAG GCG TTG GCC AAG GGA GAT GTT ACA GCC CAG ACA
 31 Lys His His Ala Ala Tyr Val Asn Asn Leu Asn Val Thr Glu Glu Lys Tyr Gln Glu Ala Leu Ala Lys Gly Asp Val Thr Ala Gln Thr

    GCT CTT CAG CCT GCA CTG AAG TTC AAT GGT GGT GGT CAT ATC AAT CAT AGC ATT TTC TGG ACA AAC CTC AGC CCT AAC GGT GGT GGA GAA
 61 Ala Leu Gln Pro Ala Leu Lys Phe Asn Gly Gly Gly His Ile Asn His Ser Ile Phe Trp Thr Asn Leu Ser Pro Asn Gly Gly Gly Glu

    CCC AAA GGG GAG TTG CTG GAA GCC ATC AAA CGT GAC TTT GGT TCC TTT GAC AAG TTT AAG GAG AAG CTG ACG GCT GCA TCT GTT GGT GTC
 91 Pro Lys Gly Glu Leu Leu Glu Ala Ile Lys Arg Asp Phe Gly Ser Phe Asp Lys Phe Lys Glu Lys Leu Thr Ala Ala Ser Val Gly Val

    CAA GGC TCA GGT TGG GGT TGG CTT GGT TTC AAT AAG GAA CGG GGA CAC TTA CAA ATT GCT GCT TGT CCA AAT CAG GAT CCA CTG CAA GGA
121 Gln Gly Ser Gly Trp Gly Trp Leu Gly Phe Asn Lys Glu Arg Gly His Leu Gln Ile Ala Ala Cys Pro Asn Gln Asp Pro Leu Gln Gly

    ACA ACA GGC CTT ATT CCA CTG CTG GGG ATT GAT GTG TGG GAG CAC GCT TAC TAC CTT CAG TAT AAA AAT GTC AGG CCT GAT TAT CTA AAA
151 Thr Thr Gly Leu Ile Pro Leu Leu Gly Ile Asp Val Trp Glu His Ala Tyr Tyr Leu Gln Tyr Lys Asn Val Arg Pro Asp Tyr Leu Lys

    GCT ATT TGG AAT GTA ATC AAC TGG GAG AAT GTA ACT GAA AGA TAC ATG GCT TGC AAA AAG CCC GGG CTC TGG GAG CGC CAG GCG CGG GAG
181 Ala Ile Trp Asn Val Ile Asn Trp Glu Asn Val Thr Glu Arg Tyr Met Ala Cys Lys Lys Pro Gly Leu Trp Glu Arg Gln Ala Arg Glu

    CAC TCA GAG CGC AAG AAG CGG CGG CGC GAG AGC GAG TGC AAG GCC GCC TAA
211 His Ser Glu Arg Lys Lys Arg Arg Arg Glu Ser Glu Cys Lys Ala Ala ---
```

Fig. 2. The nucleotide and deduced amino acid sequences of the chimeric SOD2/3. The first two residues, *MET His*, are not present in wild-type human SOD2 sequence but were introduced by the cloning strategy. Residues 2–200 (Lys His Ser . . . Cys Lys Lys) represent the exact sequence of mature wild-type human SOD2 (i.e., the sequence remaining after proteolytic cleavage of the mitochondrial signal peptide). Residues 201–226, underlined, are the COOH-terminal 26 residues from wild-type human SOD3 (Pro Gly Leu . . . Lys Ala Ala).

during this process to 10 mM potassium phosphate, 0.15 M NaCl, pH 7.4.

SDS-PAGE

Purified hrSOD2, purified hrSOD2/3, and a crude cell lysate of *E. coli* expressing mutant SOD2/3 were subjected to SDS-PAGE using a 15% gel as described (38).

Gel Filtration Chromatography

For molecular size determination, a 0.5-ml sample of the purified protein was applied to a Sephacryl S-200 column as described above but using 10 mM potassium phosphate, pH 7.4, 0.15 M NaCl instead. The column was calibrated with the protein standards aldolase (158 kDa), hrSOD2 (89.9 kDa), and hrSOD1 (31.6 kDa). Absorbance at 280 nm was monitored, and K_{av} (partition coefficient) of each standard was calculated and plotted vs. its known molecular weight.

Heparin Affinity Chromatography

An aliquot of the purified SOD2/3 preparation (500–1,000 units) was applied to a small (0.5- to 1-ml bed vol) column of heparin-agarose (Sigma) in 10 mM Tris·HCl buffer, pH 7.4. The column was washed with this buffer to remove unbound enzyme and then eluted with a gradient of 0–2.0 M NaCl. Fractions were assayed for SOD activity and for conductivity.

IL-1α-Induced Model of Pulmonary Injury

Administration of IL-1α and SODs to intact rats. This model was conducted as previously described (19). Male Sprague-Dawley rats weighing 300–350 g were anesthetized with halothane via inhalation inside of a sealed glass jar. SOD2 or the chimeric SOD2/3 was administered at the indicated dose in 0.5 ml of sterile saline via the femoral vein. Immediately after intravenous injection, the trachea was cannulated with a 24-gauge, ½-inch Teflon catheter, and 50 ng of IL-1α in 0.5 ml of sterile endotoxin-free saline was rapidly instilled intratracheally with a syringe and then followed by three 1-ml injections of air. Rats were then allowed to recover fully from anesthesia. Sham-treated rats received identical anesthesia and surgery but were injected only with sterile saline both intravenously and intratracheally.

Assessment of lung leak index. Four and one-half hours after SOD and IL-1α administration, rats were injected intravenously with 1.0 μCi of ^{125}I-BSA in a volume of 0.5 ml. Twenty minutes later, rats were ventilated by using a Harvard small animal respirator and then subjected to laparotomy, thoracotomy, and right ventricular injection of 200 units of heparin (in 0.2 ml of saline). Thirty minutes after ^{125}I injection, blood samples were obtained, lungs were perfused blood-free with phosphate buffered-saline, and lungs were excised. Right lungs and blood samples were counted in a gamma counter (Beckman, Fullerton, CA). Lung leak index was defined as counts per minute of ^{125}I in the right lung divided by counts per minute in 1.0 ml of blood.

Assessment of lung lavage and blood neutrophils. Saline (3 ml × 2) was slowly injected intratracheally and then withdrawn. Recovered lavage fluid was centrifuged for 5 min. The supernatant was carefully removed and saved. The pellet was then resuspended in 4.0 ml of water and mixed for 30 s to lyse erythrocytes. Immediately thereafter, 2.0 ml of 4 × $Ca^{2+}Mg^{2+}$-free Hanks' solution was added and mixed for 5 s. The new mixture was centrifuged again for 5 min, and the supernatant was discarded. The pellet was then resuspended in 1.0 ml of lavage supernatant. Total leukocytes were counted in a hemocytometer, and a cytospin preparation was Wright stained to determine the percentage of neutrophils.

Carrageenan-Induced Foot Edema in the Rat

This model was performed as described by Vinegar et al. (46). Edema was induced by subplantar injection of 0.1 ml of 1.5% carrageenan in saline into the foot pad. The increase in foot volume after 6 h was measured by the water displacement method (45). The saline controls received an injection of vehicle only. Native hrSOD2 or chimeric hrSOD2/3 was administered 10 min before carrageenan by intravenous injection at doses of 0.1 U/g body wt.

Statistical Analysis

All values are presented as means ± SE. Data were analyzed using the unpaired Student's *t*-test.

RESULTS

Expression and Purification of hrSOD2/3

Because the COOH-terminal SOD3-derived tail portion of the chimeric protein has been shown to be very susceptible to proteolytic degradation, we used *E. coli* UT5600 cells, a protease-deficient strain, as the host for expression of the mutant enzyme. When *E. coli* UT5600 was transformed with pGB1-*sod2/3* and cultured as described above, cell lysates contained extremely high levels of SOD activity. The major soluble protein (expressed at >20% of total protein) was of the size expected for the chimeric SOD2/3, as shown by SDS-PAGE in Fig. 3, *lane 4*. Figure 3 compares the crude lysate containing SOD2/3 (*lane 4*) with purified preparations of SOD2/3 (*lane 3*) and SOD2 (*lane 2*). Purified hrSOD2/3 (95% purity, *lane 3*) showed a single protein band with an apparent subunit molecular weight of 25–26 kDa, in agreement with the predicted molecular weight of 25,637 Da. Native hrSOD2 (with-
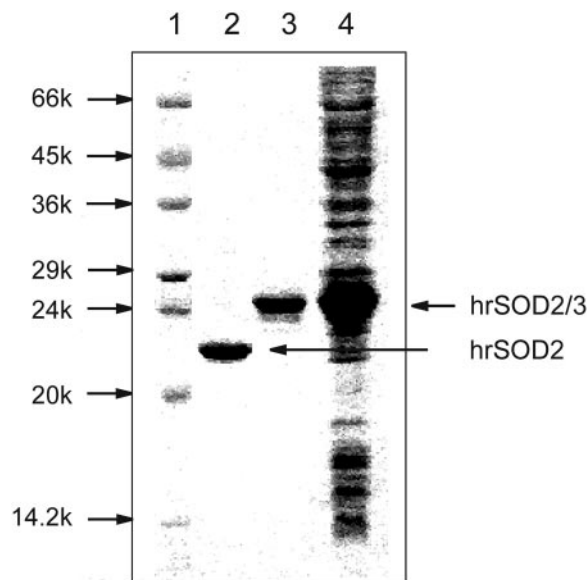

Fig. 3. SDS-PAGE of hrSOD2/3 expressed in *Escherichia coli*. *Lane 1*, molecular mass markers (kDa); *lane 2*, purified mature human recombinant (hr)SOD2; *lane 3*, purified hrSOD2/3; *lane 4*, cellular lysates of recombinants expressing SOD2/3.

Table 1. *Results of the purification of hrSOD2/3 from Escherichia coli UT5600 transformed with pGB1-sod2/3*

Purification Step	Total SOD Activity, units	Total Protein, mg	Specific Activity, U/mg	Yield
Cell lysate	427,700	881	485	100%
Supernate	404,800	600	675	95%
After heat step	345,700	328	1,054	81%
After gel filtration	284,500	173	1,647	67%
After heparin affinity chromatography	202,500	63	3,214	47%

SOD, superoxide dismutase.

out the tail) was expressed by the pGB1-*sod2* vector to slightly higher levels, as previously described (7). The subunit molecular weight of the wild-type SOD2 is shown to be 22.5 kDa (*lane 2*) for comparison purposes.

A 3-liter culture of the pGB1-*sod2/3* transformed cells was subjected to the purification procedure described in MATERIALS AND METHODS, with the results summarized in Table 1. The procedure yielded 63 mg of highly purified SOD2/3, after a purification of 6.6-fold with a yield of 47% of the starting activity. The specific activity of the purified product was 3,200 standard units/milligram of protein, comparable to the specific activity of 3,600 U/mg for SOD2 as originally isolated from human liver (26), especially if one takes into consideration the increase in molecular weight due to the additional amino acid residues comprising the SOD3 COOH-terminal region.

Gel filtration column chromatography of the hrSOD2/3 showed a molecular size of 105 kDa (Fig. 4). This value is very close to the calculated molecular weight of the tetrameric chimeric enzyme (102.6 kDa) and establishes that the tetrameric structure of native SOD2 is preserved in SOD2/3.

Heparin Binding Ability of SOD2/3

To test whether the hrSOD2/3 has a SOD3-like affinity for heparin, we performed heparin-agarose affin-

ity chromatography as described in MATERIALS AND METHODS. The results are shown on Fig. 5. The hrSOD2/3 bound to the column, eluting as a single peak at a NaCl concentration of 0.35 M. Under the same conditions, native MnSOD did not bind to the column at all (data not shown).

Effect of hrSOD2/3 on IL-1-Induced Lung Leak and Neutrophil Accumulation

We tested the ability of the hrSOD2/3 to protect rat lungs in an in vivo model of acute IL-1-induced lung injury. The model was performed as described in MATERIALS AND METHODS after IV administration of either a saline control, SOD2, or SOD2/3. Lung leak was then quantified as described. The results are shown in Fig. 6. At 0.5 mg, the chimeric enzyme suppressed the IL-1-induced lung leak by ~92% ($P < 0.026$) compared with the IL-1-treated control. In contrast, 2 mg of native SOD2 suppressed the IL-1-induced lung leak by only 13.8%, which was not statistically significant. Heat-denatured SOD2/3 did not protect at all. SOD2/3 at 2 mg also protected against the damage (79%, $P < 0.03$). As an additional index of injury, we measured neutrophils in bronchoalveolar lavage (BAL) fluid after the SOD treatments. The results are shown in Fig. 7. IL-1 administration dramatically increased the numbers of neutrophils in BAL. Although neither native SOD2 (2 mg) nor heat-denatured SOD2/3 prevented
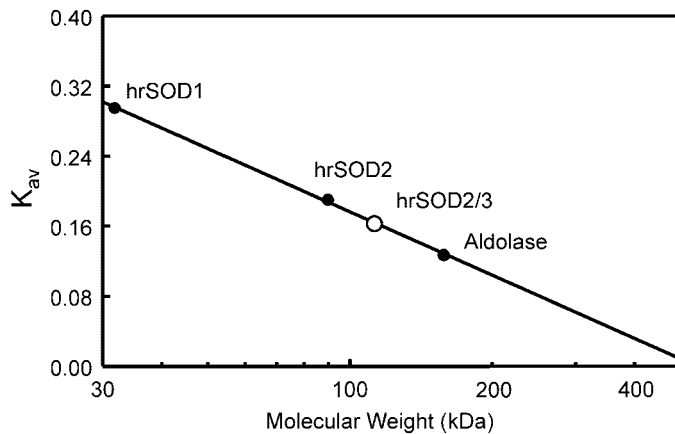

Fig. 4. Gel filtration chromatography of hrSOD2/3. Samples (0.5 ml) of human recombinant Cu,Zn-SOD (hrCu,Zn-SOD), hrMnSOD, aldolase, and hrSOD2/3 were chromatographed on a Sephacryl S-200 column as described in MATERIALS AND METHODS. Absorbance at 280 nm was monitored, and K_{av} (partition coefficient) of each sample was calculated according to the following equation: $K_{av} = V_e - V_o / V_t - V_o$. V_e is the elution volume; V_o is the void volume; V_t is the total volume of the gel bed.
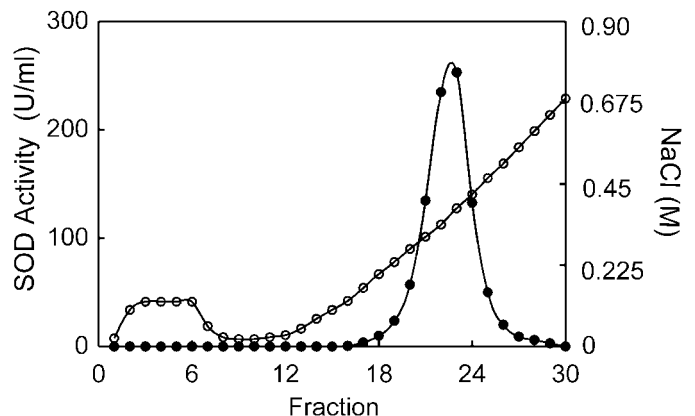

Fig. 5. Heparin-agarose column of hrSOD2/3. Chromatography was performed as described in MATERIALS AND METHODS. Fractions were collected, and SOD activity of each fraction was determined and expressed as units/ml of fraction volume. NaCl concentration was determined by conductivity of each fraction. hrSOD2/3 binds to the heparin affinity column and elutes at a NaCl concentration of ~0.35 M.
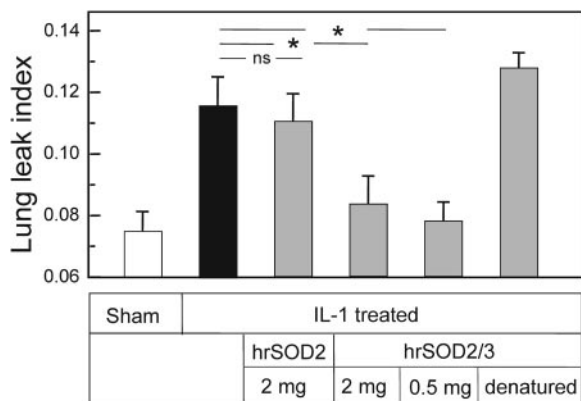
Fig. 6. hrSOD2/3 protects against IL-1-induced lung leak in rats. Lung leak was measured after intratracheal instillation of IL-1. The various SODs were intravenously administered immediately before the IL-1. *Group 1*, sham-treated rats (no IL-1); *group 2*, IL-1-treated rats; *group 3*, IL-1-treated rats pretreated with 2 mg of native hrSOD2; *group 4*, IL-1-treated rats pretreated with 2 mg of hrSOD2/3; *group 5*, IL-1-treated rats pretreated with 0.5 mg of hrSOD2/3; and *group 6*, IL-1-treated rats pretreated with 2 mg of heat-denatured hrSOD2/3. SOD2/3 suppressed the IL-1-induced lung leak by ~92% at 0.5 mg (*P < 0.03) and 79% at 2 mg (*P < 0.03) compared with the IL-1-treated control. In contrast, the protection observed by 2 mg of native MnSOD treatment was only 13.8% [not significant (ns)]. Heat-denatured SOD2/3 did not protect at all. In each group, n = 7.

this increase, SOD2/3 at 0.5 mg suppressed neutrophil accumulation by 91% (P < 0.05).

Inhibition by SOD2/3 of Carrageenan-Induced Foot Edema in the Rat

The model was carried out as described in MATERIALS AND METHODS, with the results shown in Fig. 8. After 6 h,
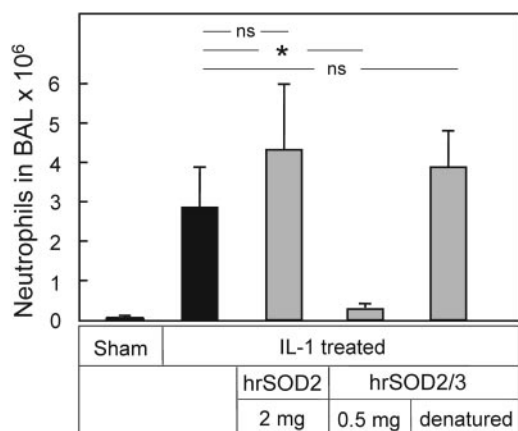

Fig. 7. hrSOD2/3 prevents polymorphonuclear neutrophil (PMN) accumulation in the IL-1-treated rat lung. PMN accumulation was measured after intratracheal instillation of IL-1. *Group 1*, sham-treated animals (no IL-1); *group 2*, IL-1-treated animals; *group 3*, IL-1-treated animals pretreated with 2 mg of native hrSOD2; *group 4*, IL-1-treated animals pretreated with 0.5 mg of hrSOD2/3; and *group 5*, IL-1-treated animals pretreated with 2 mg of heat-inactivated hrSOD2/3. IL-1 administration greatly increased the PMN in bronchoalveolar lavage (BAL). Although neither 2 mg of native hrSOD2 nor heat-inactivated hrSOD2/3 prevented this increase, 0.5 mg of active hrSOD2/3 suppressed neutrophil accumulation by 91% (*P < 0.05). For each group, n = 7.
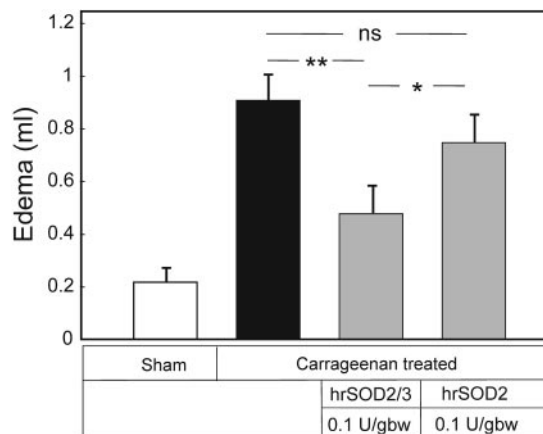

Fig. 8. Treatment of carrageenan-induced foot edema in the rat by hrSOD2 and hrSOD2/3. SOD-treated groups received the enzyme by intravenous injection at doses of 0.1 U/g body wt 10 min before administration of the carrageenan. The hrSOD2 caused a reduction in carrageenan-dependent edema of 22% (ns, n = 8) vs. untreated controls (n = 15). The hrSOD2/3 caused a 62% reduction in edema (P < 0.003, n = 9). *P < 0.05; **P < 0.003. For the sham-injected group, n = 3.

sham (saline)-injected feet showed a volume increase of 0.2 ml, only slightly larger than the actual volume injected (n = 3). Carrageenan-injected feet receiving no SOD treatment showed an average edema of ~0.9 ml (n = 15). Pretreatment of animals with chimeric SOD2/3 at 0.1 U/g body wt (n = 9) resulted in a 62% reduction of carrageenan-dependent edema (P < 0.003). Pretreatment of animals with native SOD2 at the same dosage (n = 8) produced a 22% reduction of carrageenan-dependent edema that was not statistically significant.

DISCUSSION

For more than 30 yr, there have been attempts to use SOD as a therapeutic agent to treat conditions known to involve the production of the superoxide radical, such as inflammation, fibrosis, and ischemia-reperfusion. Although there have been impressive results in laboratory models, the human clinical experience has been less than spectacular. Over time, the reasons for this paradox have become clear. Nearly all the clinical trials have utilized SOD1 (mostly human recombinant or bovine) because of its commercial availability, stability, economy, ease of purification, and low immunogenicity. Despite these attractive features, however, the SOD1 protein displays some unfortunate physiological characteristics that render it poorly suited for therapeutic use. Perhaps the greatest problem is that native SOD1 (molecular radius in the short dimension of only 15 Å) has a plasma half-life of only ~10 min due to rapid renal clearance (2), whereas SOD2 (molecular radius of ~40 Å, near neutral charge) has a half-life of 4–20 h, depending on species (1), and SOD3 has a slow clearance, with a half-life of ~10 h in the rabbit (17). (It is actually not possible to measure a true plasma clearance rate for a protein that is not present in the plasma. Both SOD3 and SOD2/3 immediately bind to

surfaces, so analysis of a plasma sample does not reflect how much of the proteins remain in the body.) We have shown that maintaining an appropriate dose of SOD is critical due to bell-shaped dose-response curves (34, 35) resulting from the facts that superoxide radical can paradoxically both initiate and terminate lipid peroxidation (32) and is involved in a number of cell signaling pathways (25). Hence, a unique concentration of SOD is maximally protective for any given level of oxidative stress, and maintaining this concentration in practice becomes extremely difficult for a protein with a plasma half-life of 10 min. Thus an SOD with a slow plasma clearance should be greatly superior to one that is rapidly cleared, like human SOD1.

In addition, we have shown that the negatively charged human SOD1 (net charge per subunit of −6.1 at pH 7.4) equilibrates rather slowly between vascular and interstitial spaces, whereas the nearly uncharged MnSOD (net charge per subunit of −0.85 at pH 7.4) equilibrates four times faster (36) despite its larger size. Earlier work had revealed that SODs carrying a net positive charge were as much as two orders of magnitude more effective in protecting phagocytosing neutrophils from superoxide-mediated self-destruction than were negatively charged SODs (29). This was thought to be due to the fact that cell surfaces are negatively charged, and an uncharged or positively charged SOD might approach cell surfaces more easily by elimination of electrostatic repulsion forces. In fact, a positively charged SOD might be attracted to such surfaces and might even bind to them. We previously tested this hypothesis by covalently attaching polylysine polymers to bovine SOD1, such that each subunit, on average, possessed a tail of about a dozen lysine residues. This polylysyl-SOD1 derivative was ~10-fold better at protecting cells from oxidative stress-induced death than the native SOD1 (29). The subsequent discovery of SOD3 by Marklund and colleagues (13, 20) suggested that nature had used the same design for protecting external cell surfaces. SOD3 subunits possess COOH-terminal tails of ~22 hydrophilic amino acid residues with a strong net positive charge, very much like the polylysyl-SOD1 that we had synthesized. Also noteworthy is the fact that the SOD3 tail terminates with the sequence -ala-ala-COOH. Any sequence terminating with the basic residues arginine or lysine would be rapidly nibbled away by plasma carboxypeptidases, but the ala-ala cap resists such hydrolysis.

Thus it seemed likely that SOD3 would be a much better therapeutic candidate than SOD1, and we wanted to reexamine the therapeutic potential of SOD in the various physiological models, but using SOD3 instead of SOD1. Attempts to produce large quantities of hrSOD3 in bacterial or yeast hosts were thwarted by the difficulty for these hosts to express the recombinant protein (11). The reason for this is unclear. In any event, we decided to construct a chimeric gene that would produce a hybrid SOD combining the desirable properties gleaned from all the studies described above. The ideal theoretical size might be a molecular radius of 45–50 Å to discourage filtration by the kid-

neys but still allow egress from the vasculature to equilibrate with interstitial fluid. The chimeric enzyme would be based on human SOD2, the least negatively charged of the three SOD isoenzymes. It is tetrameric with a molecular radius of ~40 Å; the addition of the 24-residue tail to each subunit would put SOD2/3 in the desired size range with a radius of 45–50 Å. SOD1 is rather asymmetric, but in its narrow orientation has a molecular radius of only ~15 Å, accounting for its rapid renal clearance. By attaching the COOH-terminal 24 residues of SOD3 to SOD2, a net positive charge would be created along with four binding sites for polyanionic surfaces such as heparin or heparan sulfate, or for collagen fibrils and other components of the extracellular matrix (37). Thus the chimeric enzyme SOD2/3 might actually have more desirable properties from a therapeutic point of view than any of the three naturally occurring forms of SOD. Construction of other chimeric SODs have been described by Inoue et al. (14, 15) and by Stenlund and Tibell (42). Inoue et al. (14, 15) combined the human SOD1 cDNA and that portion of the human SOD3 DNA encoding the final 26 COOH-terminal residue tail. This construct produced an SOD that bound to heparin (HB-SOD) but retained a net negative charge on its surface and an undesirably small molecular radius. Although this enzyme did not quickly appear in the urine, it was largely retained in the kidney (37% after 20 min) through binding to the apical plasma membrane of tubular cells (14). This HB-SOD possessed better therapeutic properties than native SOD1 (31) but fell short of achieving optimal characteristics. The chimeric enzyme constructed by Stenlund and Tibell consisted of SOD1 with both NH2-terminal and COOH-terminal regions of SOD3. The NH2-terminal sequence produces the tetrameric interface of SOD3 such that this chimeric enzyme behaves much like true SOD3. There have been no published assessments of its therapeutic characteristics.

A comparison of net surface charges borne by the three wild-type human SODs and for two heparin-binding chimeric SODs at pH 7.4 is shown in Fig. 9. Calculations were made by using PC Gene software and the sequence
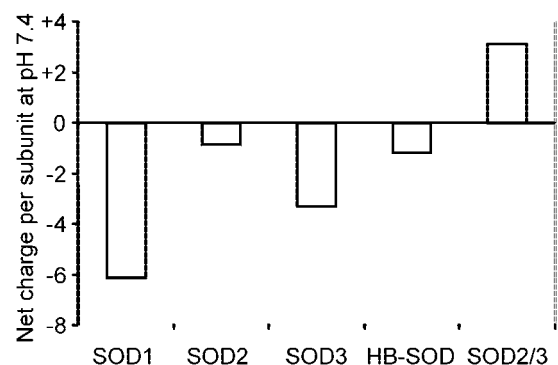

Fig. 9. A comparison of net charges borne by the 3 wild-type human SODs and for 2 heparin-binding mutant SODS at pH 7.4. Calculations were made by using PC Gene software (IntelliGenetics) and the sequence data for the various proteins. HB-SOD consists of human SOD1 plus the 26 COOH-terminal residues of extracellular-SOD as described by Inoue et al. (15).

data for the various proteins. Of these five SOD preparations, only SOD2/3 bears a net positive surface charge, shown by us to be essential for rapid equilibration between vascular and interstitial compartments (36).

Although native SOD3 clearly has an affinity for vascular endothelial surfaces and may be displaced by heparin (16), SOD3 has been found in much greater amounts bound to components such as type 1 collagen fibrils in the extracellular matrix in lung (37) and the arterial wall interstitium (43) and has been shown to be synthesized and secreted in large amount by arterial smooth muscle cells. These observations raise the question of how diffusible SOD3 is in a normal individual; it may not freely equilibrate between vascular and interstitial spaces or from tissue to tissue. This could be due to size and charge characteristics that impede the equilibration of SOD3 across the plasma-interstitium barrier or it could be due to the very tight binding of SOD3 to polyanionic surfaces producing a very slow equilibration. Native SOD3 elutes from heparin-agarose at a salt concentration of $\sim$0.55 M. A common variant form of SOD3 (arg213gly) found in 2–5% of the population binds less tightly due to the replacement of an arginine residue in the tail region of the enzyme. Karlsson et al. (18) have speculated that the reason this mutation is so common may be that it is more mobile than the native SOD3, possibly conveying an advantage under certain pathological circumstances (40). SOD2/3 elutes from a heparin-agarose column at a NaCl concentration of 0.35 M (see Fig. 5), about the same as the mutant form of SOD3. This slightly weaker binding than wild-type SOD3 was not expected because SOD2/3 has a net positive charge and the tail sequences are identical. It may be due to different spatial presentations of the tails in the two proteins. For whatever reasons, this weaker binding, which resulted by happenstance rather than by design, may contribute to making SOD2/3 a better therapeutic agent than SOD3.

As a physiological model of oxidative injury, we used intratracheal IL-1 instillation followed by measurements of lung leak and neutrophil infiltration. We have previously shown (19) that SOD2 at 2 mg/rat can provide modest but significant protection against both end points, although in the present study, statistical significance was not achieved. The chimeric SOD2/3, however, provided essentially complete suppression of both neutrophil migration and the lung leak caused by the IL-1 and was just as effective when the dosage was decreased by 75% (Figs. 6 and 7). The only difference between the mutant and the native enzymes is the presence of the heparin-binding tail. Thus we can conclude that the ability to bind to endothelial cell surfaces and to extracellular matrix components provides a dramatic advantage in protecting against IL-1-induced lung damage.

The second in vivo model tested, the carrageenan-induced foot edema model, is widely used to assess anti-inflammatory agents. Rats were dosed at the remarkably low dose of 0.1 U/g body wt (or 30 μg/kg), administered intravenously, 10 min before the injection of carrageenan into the footpad. The native SOD2 caused a modest reduction in carrageenan-dependent edema that was not

statistically significant. The chimeric SOD2/3, however, caused a 62% reduction in edema ($P < 0.003$), approximately equal to the effects of hydrocortisone or phenylbutazone at dosages of 50 mg/kg (46).

The effectiveness of SOD2/3 in the two models examined, over a 200-fold-dose range, suggests that this engineered enzyme may have great advantages over SOD1, SOD2, and even SOD3, when used in vivo as a therapeutic agent. We have also utilized the chimeric enzyme in a model of ischemia-reperfusion injury in the isolated rabbit heart, finding it $\sim$75-fold more efficacious than SOD2 in providing recovery of developed ventricular pressure, prevention of lipid peroxidation, and prevention of lactate dehydrogenase release during reperfusion (33). It was similarly protective in a cold ischemia preservation model (33). These isolated organ studies showed rather sharp bell-shaped dose response curves, not suggested in the present studies conducted in vivo. A possible explanation might be the "buffering" of the SOD2/3 concentration by the large binding capacity provided by the rest of the animal's body. Further dose-response studies are needed to explore this possibility.

The chimeric SOD2/3 has also been shown to effectively prevent the adherence of platelets to vascular endothelial cells in response to bacterial endotoxin (4). This study was performed in vivo in the mouse at an intravenous dose of 2 U/g body wt (600 ng/g body wt). In a mouse model of hepatic ischemia-reperfusion, the chimeric SOD2/3 at an intravenous dose of 1 U/g body wt (300 ng/g body wt) provided complete suppression of serum TNF-α protein expression after 45 or 90 min of ischemia and 6 h of reperfusion, whereas the native SOD2 at the same dosage provided no effect at all (12).

In summary, we believe that this chimeric form of SOD possesses pharmacological properties that are superior to any of the three naturally occurring forms of the human enzyme. By mimicking the ability of extracellular SOD3 to bind to cell surfaces and components of the extracellular matrix, thereby buffering the effective concentration in vivo, the enzyme appears to overcome the major problems that have prevented the translation of superoxide-scavenging therapies from the laboratory to human clinical practice.

REFERENCES

1. **Baret A, Jadot G, and Michelson AM.** Pharmacokinetic and anti-inflammatory properties in the rat of superoxide dismutases (Cu SODs and Mn SOD) from various species. *Biochem Pharmacol* 33: 2755–2760, 1984.
2. **Bayati A, Källskog Ö, Odlind B, and Wolgast M.** Plasma elimination kinetics and renal handling of copper/zinc superoxide dismutase in the rat. *Acta Physiol Scand* 134: 65–74, 1988.
3. **Carlioz A and Touati D.** Isolation of superoxide dismutase mutants in *Escherichia coli*: is superoxide dismutase necessary for aerobic life? *EMBO J* 5: 623–630, 1986.
4. **Cerwinka WH, Cooper D, Krieglstein CF, Ross CR, McCord JM, and Granger DN.** Superoxide mediates endotoxin-

induced platelet-endothelial cell adhesion in intestinal venules. *Am J Physiol Heart Circ Physiol* 284: H535–H541, 2003.

5. **Crapo JD, McCord JM, and Fridovich I.** Superoxide dismutases: preparation and assay. *Methods Enzymol* 53: 382–393, 1978.

6. **Elish ME, Pierce JR, and Earhart CF.** Biochemical analysis of spontaneous fepA mutants of *Escherichia coli*. *J Gen Microbiol* 134: 1355–1364, 1988.

7. **Gao B, Flores SC, Bose SK, and McCord JM.** A novel *Escherichia coli* vector for oxygen-inducible high level expression of foreign genes. *Gene* 176: 269–272, 1996.

8. **Granger DN, Rutili G, and McCord JM.** Superoxide radicals in feline intestinal ischemia. *Gastroenterology* 81: 22–29, 1981.

9. **Hanahan D.** Studies on transformation of *Escherichia coli* with plasmids. *J Mol Biol* 166: 557–580, 1983.

10. **Hatori N, Sjoquist PO, Marklund SL, Pehrsson SK, and Ryden L.** Effects of recombinant human extracellular-superoxide dismutase type-c on myocardial reperfusion injury in isolated cold-arrested rat hearts. *Free Radic Biol Med* 13: 137–142, 1992.

11. **He HJ, Yuan QS, Yang GZ, and Wu XF.** High-level expression of human extracellular superoxide dismutase in *Escherichia coli* and insect cells. *Protein Expr Purif* 24: 13–17, 2002.

12. **Hines IN, Hoffman JM, Scheerens H, Day BJ, Harada H, Pavlick KP, Bharwani S, Wolf R, Gao B, Flores S, McCord JM, and Grisham MB.** Regulation of postischemic liver injury following different durations of ischemia. *Am J Physiol Gastrointest Liver Physiol* 284: G536–G545, 2003.

13. **Hjalmarsson K, Marklund SL, Engstrom A, and Edlund T.** Isolation and sequence of complementary DNA encoding human extracellular superoxide dismutase. *Proc Natl Acad Sci USA* 84: 6340–6344, 1987.

14. **Inoue M, Watanabe N, Matsuno K, Sasaki J, Tanaka Y, Hatanaka H, and Amachi T.** Expression of a hybrid Cu/Zn-type superoxide dismutase which has high affinity for heparin-like proteoglycans on vascular endothelial cells. *J Biol Chem* 266: 16409–16414, 1991.

15. **Inoue M, Watanabe N, Morino Y, Tanaka Y, Amachi T, and Sasaki J.** Inhibition of oxygen toxicity by targeting superoxide dismutase to endothelial cell surface. *FEBS Lett* 269: 89–92, 1990.

16. **Karlsson K and Marklund SL.** Heparin-induced release of extracellular superoxide dismutase to human blood plasma. *Biochem J* 242: 55–59, 1987.

17. **Karlsson K and Marklund SL.** Plasma clearance of human extracellular-superoxide dismutase C in rabbits. *J Clin Invest* 82: 762–766, 1988.

18. **Karlsson K, Sandstrom J, Edlund A, Edlund T, and Marklund SL.** Pharmacokinetics of extracellular-superoxide dismutase in the vascular system. *Free Radic Biol Med* 14: 185–190, 1993.

19. **Leff JA, Baer JW, Bodman ME, Kirkman JM, Shanley PF, Patton LM, Beehler CJ, McCord JM, and Repine JE.** Interleukin-1-induced lung neutrophil accumulation and oxygen metabolite-mediated lung leak in rats. *Am J Physiol Lung Cell Mol Physiol* 266: L2–L8, 1994.

20. **Marklund SL.** Human copper-containing superoxide dismutase of high molecular weight. *Proc Natl Acad Sci USA* 79: 7634–7638, 1982.

21. **Marklund SL.** Extracellular superoxide dismutase and other superoxide dismutase isoenzymes in tissues from nine mammalian species. *Biochem J* 222: 649–655, 1984.

22. **Marklund SL.** Properties of extracellular superoxide dismutase from human lung. *Biochem J* 220: 269–272, 1984.

23. **McCord JM.** Oxygen-derived free radicals in post-ischemic tissue injury. *N Engl J Med* 312: 159–163, 1985.

24. **McCord JM.** Superoxide production and human disease. In: *Molecular Basis of Oxidative Damage by Leukocytes*, edited by Jesaitis A and Dratz E. Boca Raton, FL: CRC, 1992, p. 225–239.

25. **McCord JM.** The evolution of free radicals and oxidative stress. *Am J Med* 108: 652–659, 2000.

26. **McCord JM, Boyle JA, Day ED Jr, Rizzolo LJ, and Salin ML.** A manganese-containing superoxide dismutase from human liver. In: *Superoxide and Superoxide Dismutase*, edited by Michelson AM, McCord JM, and Fridovich I. London: Academic, 1977, p. 129–138.

27. **McCord JM and Fridovich I.** Superoxide dismutase: an enzymic function for erythrocuprein (hemocuprein). *J Biol Chem* 244: 6049–6055, 1969.

28. **McCord JM, Gao B, Leff J, and Flores SC.** Neutrophil-generated free radicals: possible mechanisms of injury in adult respiratory distress syndrome. *Environ Health Perspect* 102: 57–60, 1994.

29. **McCord JM and Salin ML.** Self-directed cytotoxicity of phagocyte-generated superoxide free radical. In: *Movement, Metabolism and Bactericidal Mechanisms of Phagocytes,* edited by Rossi F, Patriarca P, and Romeo D. Padova, Italy: Piccin Medical Books, 1977, p. 257–264.

30. **McCord JM and Wong K.** Phagocyte-produced free radicals: roles in cytotoxicity and inflammation. In: *Oxygen Free Radicals and Tissue Damage*, edited by Ciba Foundation Symposium 65 (new series). Amsterdam: Excerpta Medica, 1979, p. 343–360.

31. **Nakazono K, Watanabe N, Matsuno K, Sasaki J, Sato T, and Inoue M.** Does superoxide underlie the pathogenesis of hypertension. *Proc Natl Acad Sci USA* 88: 10045–10048, 1991.

32. **Nelson SK, Bose SK, and McCord JM.** The toxicity of high-dose superoxide dismutase suggests that superoxide can both initiate and terminate lipid peroxidation in the reperfused heart. *Free Radic Biol Med* 16: 195–200, 1994.

33. **Nelson SK, Gao B, Bose SK, Rizeq M, and McCord JM.** A novel mutant human Mn-superoxide dismutase improves myocardial preservation and protects from ischemia/reperfusion injury. *J Heart Lung Transplant* 21: 1296–1303, 2002.

34. **Omar BA, Gad NM, Jordan MC, Striplin SP, Russell WJ, Downey JM, and McCord JM.** Cardioprotection by Cu,Zn-superoxide dismutase is lost at high doses in the reoxygenated heart. *Free Radic Biol Med* 9: 465–471, 1990.

35. **Omar BA and McCord JM.** The cardioprotective effect of Mn-superoxide dismutase is lost at high doses in the postischemic isolated rabbit heart. *Free Radic Biol Med* 9: 473–478, 1990.

36. **Omar BA and McCord JM.** Interstitial equilibration of superoxide dismutase correlates with its protective effect in the isolated rabbit heart. *J Mol Cell Cardiol* 23: 149–159, 1991.

37. **Oury TD, Chang LY, Marklund SL, Day BJ, and Crapo JD.** Immunocytochemical localization of extracellular superoxide dismutase in human lung. *Lab Invest* 70: 889–898, 1994.

38. **Sambrook J, Fritsch TM, and Maniatis T.** *Molecular Cloning. A Laboratory Manual*. Cold Spring Harbor, NY: Cold Spring Harbor Laboratory, 1989.

39. **Sandstrom J, Carlsson L, Marklund SL, and Edlund T.** The heparin-binding domain of extracellular superoxide dismutase C and formation of variants with reduced heparin affinity. *J Biol Chem* 267: 18205–18209, 1992.

40. **Sandstrom J, Nilsson P, Karlsson K, and Marklund SL.** 10-fold increase in human plasma extracellular superoxide dismutase content caused by a mutation in heparin-binding domain. *J Biol Chem* 269: 19163–19166, 1994.

41. **Sjöquist P-O, Carlsson L, Jonason G, Marklund SL, and Abrahamsson T.** Cardioprotective effects of recombinant human extracellular superoxide dismutase type C in rat isolated heart subjected to ischemia and reperfusion. *J Cardiovasc Pharmacol* 17: 678–683, 1991.

42. **Stenlund P and Tibell LA.** Chimeras of human extracellular and intracellular superoxide dismutases. Analysis of structure and function of the individual domains. *Protein Eng* 12: 319–325, 1999.

43. **Stralin P, Karlsson K, Johansson BO, and Marklund SL.** The interstitium of the human arterial wall contains very large amounts of extracellular superoxide dismutase. *Arterioscler Thromb Vasc Biol* 15: 2032–2036, 1995.

44. **Tibell L, Hjalmarsson K, Edlund T, Skogman G, Engstrom A, and Marklund S.** Expression of human extracellular superoxide dismutase in Chinese hamster ovary cells and characterization of the product. *Proc Natl Acad Sci USA* 84: 6634–6638, 1987.

45. **Vinegar R.** Quantitative studies concerning kaolin edema formation in rats. *J Pharmacol Exp Ther* 161: 389–395, 1968.

46. **Vinegar R, Schreiber W, and Hugo R.** Biphasic development of carrageenan edema in rats. *J Pharmacol Exp Ther* 166: 96–103, 1969.